Ionization potentials and structural properties of finite-length single-walled carbon nanotubes: DFT study

ARTICLE *in* PHYSICA E LOW-DIMENSIONAL SYSTEMS AND NANOSTRUCTURES · DECEMBER 2013

Impact Factor: 2 · DOI: 10.1016/j.physe.2013.07.004

2 AUTHORS:

Igor K Petrushenko
Irkutsk State Technical University
15 PUBLICATIONS **39** CITATIONS
SEE PROFILE

Nikolai Ivanov
Irkutsk State Technical University
15 PUBLICATIONS **39** CITATIONS
SEE PROFILE

Physica E 54 (2013) 262–266

Contents lists available at ScienceDirect

Physica E

journal homepage: www.elsevier.com/locate/physe

Ionization potentials and structural properties of finite-length single-walled carbon nanotubes: DFT study

Igor K. Petrushenko *, Nikolay A. Ivanov

Physical and Technical Institute, Irkutsk State Technical University, 83 Lermontov Street, 664074 Irkutsk, Russia

HIGHLIGHTS

- We calculated vertical and adiabatic ionization potentials for a series of SWCNTs.
- The SWCNTs aromaticity influence on ionization potentials was observed.
- We examine changes in the structure of SWCNTs upon ionization.

ARTICLE INFO

Article history:
Received 19 December 2012
Received in revised form
1 July 2013
Accepted 9 July 2013
Available online 18 July 2013

Keywords:
Single-walled carbon nanotube
Ionization potential
DFT
B3LYP

ABSTRACT

Adiabatic and vertical ionization potentials (IPs) of single-walled carbon nanotubes (SWCNTs) as a function of length were determined by using density functional theory. The correlation between periodic oscillations of SWCNTs local aromaticity and the values of IPs was founded. In the case of short SWCNTs an appreciable gap between vertical and adiabatic IPs was observed, whereas for longer nanotubes these values are almost equal. It was also established that the HOMO electron density distribution in neutral SWCNTs affects on SWCNT lengths upon ionization.

1. Introduction

The researches focusing on single-walled carbon nanotubes (SWCNTs) [1] are great challenge to scientists worldwide. The last two decades were the period of extensive studies of SWCNTs both theoretically and experimentally. Unique structural, mechanical, electrical, physical and chemical properties were studied in detail [2–10].

Surprisingly, ionized nanotubes have not received much attention. There are a few papers, in our knowledge, devoted to such investigations. The comprehensive work of Zhou et al. [11] reveals the electronic properties of pristine armchair SWCNTs. In that paper, ionization potential (IP) and electron affinity (EA), symmetry of nanotubes and their molecular orbitals, polarizability of many model systems were studied. The work of Buonocore et al. [12] focuses on IP and EA determination of both pristine SWCNTs and arrays of SWCNTs. However, in that paper, the authors did not state which types of IP and EA, vertical (IP_v, EA_v) or adiabatic (IP_a, EA_a), were discussed. Buzatu et al. [13], although calculated IPs of nanotubes, made no mention of their types. Undoubtedly, the difference between vertical and adiabatic IPs is commonly slight, but it is of no use to mix up these two concepts. Baldoni et al. [14] and Galano [15] used Koopmans' theorem to calculate IPs of armchair SWCNTs, besides in the latter work it was made by semi-empirical PM3 technique. Furthemore, Szakács et al. [16] theoretically studied Jahn–Teller distortion of ionized and excited SWCNTs. In the Murzashev's work [17], it was established that the excess charge in ionized carbon nanotubes is distributed non-uniformly along their length. We can see that a huge lump of papers on various SWCNTs properties has been issued, but IPs and EAs attracted little attention. However, we should emphasize that the transition of nanotubes from neutral to radical cation state is closely connected with remarkable changes in electron structure, which, in turn, enhance the reactivity. Such an activation expands the limits of organic synthesis; it allows obtaining aim products selectively, more efficiently, and under non-rigid conditions.

The short list of papers above mentioned witnesses that there exists a demand for profound investigations of IP_v and IP_a of nanotubes. Also, it is worth to study structural changes that arise

* Corresponding author. Tel./fax: +7 3952 405900.
E-mail addresses: igor.petrushenko@istu.edu, igor.phd@yandex.ru (IK. Petrushenko).

1386-9477/$ - see front matter © 2013 Published by Elsevier B.V.
http://dx.doi.org/10.1016/j.physe.2013.07.004

in ionized SWCNTs, because it seems that the removal of an electron from a molecular orbital causes major changes in the framework of SWCNTs. To the best of our knowledge, there are no papers dealt with this problem.

Motivated by the above considerations, in this article we study the electronic and structural properties of armchair SWCNTs by techniques based on density functional theory (DFT), which has been successfully applied to predict many SWCNT properties with high reliability and less computational efforts than the majority of the traditional *ab initio* methods. The emphasis of this work is on structures of a series of finite-length uncapped SWCNTs and their radical cations.

2. Computational details

The models $C_{20n}H_{20}$ were used as neutral armchair nanotubes, where $n=2$–10. The model $C_{40}H_{20}$ was chosen as the shortest carbon nanotube according to [18]. In that work, the hoop-shaped cyclophenacene $C_{60}Me_5Ph_5H_2$, containing the $C_{40}H_{20}$ fragment, was synthesized for the first time. In the present discussion a SWCNT is considered "short" if it consists of 40–100 carbon atoms, and "long", if it consists of 120–200 carbon atoms.

The ends of all studied models were passivated with hydrogen atoms to avoid the dangling. Orca 2.8 [19] molecular modeling software was used to perform DFT calculations on the investigated systems. Calculations were carried out using gradient corrected DFT with Becke's three-parameter hybrid exchange functional and the Lee–Yang–Parr correlation functional (B3LYP) [20,21]. As is well-known B3LYP functional was employed in many research works on nanotubes and their properties, for example [11,18,22]. Moreover, the B3LYP results agree well with those obtained by ab initio MP2 [23]. In order to calculate equilibrium geometries of studied structures, we used SVP (split-valence polarization) basis set, which is equivalent to the commonly used 6-31G* basis set [24]. In SVP the inner shell atomic orbitals are described by a single basis function, two basis functions are provided for each valence shell atomic orbital, augmented by a set of polarization functions. To reduce the time of calculations we used the resolution of identity (RI) option [25,26].

The IPs_a of the SWCNTs were determined by applying the following procedures. The total energies of a neutral nanotube and a +1 charge radical cation ($SWCNT^{\bullet+}$) of the same tube were calculated at the B3LYP/SVP level. The ionization energy was then obtained by subtracting the total energy of the neutral nanotube from the energy of the +1 charge nanotube radical cation

$$IP_a = E(SWCNT^{\bullet+}) - E(SWCNT)$$

In order to obtain IPs_v, we calculated the total energies of the ionic states of each SWCNT, using the optimized geometry of the neutral system, then we subtracted the total energy of the neutral nanotube from the energy of the radical cation of SWCNT obtained at the geometry of neutral

$$IP_v = E(SWCNT_n^{\bullet+}) - E(SWCNT)$$

where $E(SWCNT_n^{\bullet+})$ is the total energy computed at the same equilibrium geometry as neutral SWCNT.

3. Results and discussion

With acquired information concern IP_a and IP_v, we compared two series of values from Table 1.

Since the relaxed geometry of radical cation $SWCNT^{\bullet+}$, is sure, of lower energy than its unrelaxed geometry corresponding to neutral SWCNT, $IP_v > IP_a$ for all studied SWCNTs. Although the difference between IP_v and IP_a seems very moderate and in the case of "long" tubes it tends to be zero, we must separate these two definitions of IPs, because two different scenarios are in the basis of these definitions. Examining infinite tubes, we are very likely can use any IP definition. Unfortunately, previously mentioned authors did not state clearly whether their values are adiabatic or vertical [12,13,15]. The remarkable exceptions are the works [11,14]. On the one hand, it is quite unreasonable to compare directly our IPs predictions and literature data. On the other hand, we can compare our results with those obtained from DFT calculations [11,12,18] (Table 2) as well as general trends in changing of IPs with outcomes of papers [11,12].

It should be noted, the Matsuo's et al. work [18] presents only HOMO energies, therefore, using Koopmans' theorem, one can obtain only rough approximations of IP values for a series of SWCNTs.

The observation to be made is that both IP_a and IP_v exhibit an oscillation on increasing the nanotube length (Table 1). The oscillating behavior of both IP types coincides completely with

Table 1
Properties of optimized (5,5) SWCNT fragments as described in the paper.

SWCNT	Network	Length (SWCNT) (Å)	Length ($SWCNT^{\bullet+}$) (Å)	ΔL (Å)	IP_a (eV)	IP_v (eV)	E (HOMO) (eV)
$C_{40}H_{20}$	K	3.656	3.683	0.027	6.13 (5.96)[a] (5.9)[b]	6.24	−5.034
$C_{60}H_{20}$	C	6.100	6.117	0.017	5.35 (5.17)[a] (5.6)[b]	5.43	−4.349
$C_{80}H_{20}$	iC	8.607	8.593	−0.014	5.43 (5.24)[a] (5.7)[b]	5.48	−4.480
$C_{100}H_{20}$	K	11.056	11.073	0.017	5.38 (5.23)[a] (5.2)[b]	5.44	−4.532
$C_{120}H_{20}$	C	13.507	13.518	0.011	4.98 (4.81)[a] (5.3)[b]	5.00	−4.159
$C_{140}H_{20}$	iC	16.013	15.997	−0.016	5.20 (4.99)[a] (5.2)[b]	5.24	−4.425
$C_{160}H_{20}$	K	18.461	18.475	0.014	5.06 (4.82)[a] (4.9)[b]	5.10	−4.350
$C_{180}H_{20}$	C	20.970	20.952	−0.018	4.86 (4.65)[a]	4.89	−4.181
$C_{200}H_{20}$	iC	23.418	23.400	−0.018	5.07 (4.91)[a]	5.09	−4.423

C—complete Clar network; iC—incomplete Clar network; K—Kekule network; ΔL=length ($SWCNT^{\bullet+}$)−length (SWCNT).

[a] Ref. [11].

[b] Ref. [12].

Table 2
IP_a and IP_v values vs. nanotube length.

SWCNT	IP_a, IP_v (eV)[11]	IP (eV) [12]	IP (eV) [18]
$C_{40}H_{20}$	5.96, 6.07	5.9	7.80
$C_{60}H_{20}$	5.17, 5.27	5.6	7.10
$C_{80}H_{20}$	5.24, 5.28	5.7	7.25
$C_{100}H_{20}$	5.23, 5.25	5.2	7.25
$C_{120}H_{20}$	4.81, 4.83	5.3	6.85
$C_{140}H_{20}$	4.99, 5.00	5.2	7.10
$C_{160}H_{20}$	4.82, 4.90	4.9	7.10
$C_{180}H_{20}$	4.65, 4.68	–	6.75
$C_{200}H_{20}$	–, 4.91	–	7.00

results of Zhou et al. (Tables 1 and 2). The IP_a and IP_v values also show very good correlation. When comparing with Matsuo's et al. results, we can observe the similarity in trends of IP changing, although the results obtained by the usage of Koopmans' theorem demonstrate a clear overestimation of IPs. Buonocore's et al. results for "long" tubes [12], strangely, show opposite behavior; their IP values are in antiphase with ours (Table 2). The general similarity of all reviewed papers is the decrease in values of IPs for "long" nanotubes.

In an attempt to gain some insight into the nature of these oscillations, we employed Matsuo's et al. concept, which described elsewhere [18]. Briefly, they proposed that the structure of SWCNTs and their local aromaticity oscillate periodically to generate three structures: a Kekule network, an incomplete Clar, and complete Clar networks as the SWCNT is elongated by step-by-step layering (Fig. 1).

Fig. 1 shows the schematic view of three studied nanotubes ($C_{40}H_{20}$, $C_{60}H_{20}$, $C_{80}H_{20}$) as an example. $C_{40}H_{20}$ can be regarded as Kekule structure (Fig. 1A). Addition of 20 carbon atoms to $C_{40}H_{20}$ creates $C_{60}H_{20}$, where two cyclic arrays of Clar structures can be identified (Fig. 1B). Another layer of carbon atoms produces $C_{80}H_{20}$ where two cyclic arrays of Clar structures can be clearly seen and the edge double bonds are isolated from the Clar network and are quite short (Fig. 1C). Progression from $C_{40}H_{20}$ to $C_{80}H_{20}$ completes the first period of the structural oscillation in a series of investigated nanotubes.

In the second column of Table 1 the types of networks corresponded to SWCNTs under study were listed. We could also establish some periodicity of IP values changing. It appears that the highest IPs correspond to a Kekule network, the lowest to a Clar network, and the average values to an incomplete Clar network. The latter was characterized by Clar structures (i.e. pure benzene) which were double-sided enclosed by alkene-like species. The simple explanation of the excess of IPs corresponded to an incomplete Clar network over the IPs corresponded to a complete Clar network is a matter of general knowledge, namely, the simplest alkene has bigger IP than the simplest aromatic hydrocarbon, therefore we may proved qualitatively the above mentioned. The greater IP values of SWCNTs with a Kekule network are hard to explain, but we, probably, should take into consideration that double C–C bonds are on the both ends of these

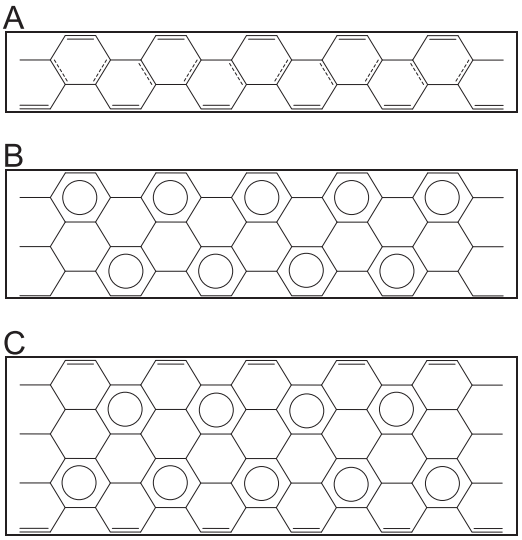

Fig. 1. Schematic structures of finite-length SWCNTs. Chemical bonds are represented by using single-bond (solid single line; bond length > 1.43 Å), double-bond (solid double line; bond length < 1.38 Å), single-bond halfway to double-bond (solid-dashed line; 1.43 Å $>$ bond length > 1.38 Å), and Clar structures (ideal benzene). Hydrogen atoms are omitted for clarity. (A) $C_{40}H_{20}$, (B) $C_{60}H_{20}$ and (C) $C_{80}H_{20}$.

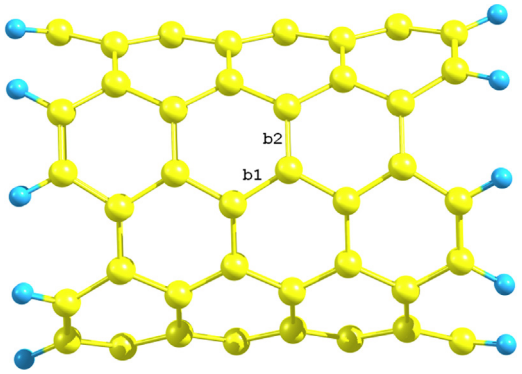

Fig. 2. Optimized structure of $C_{80}H_{20}$ SWCNT (the back side is omitted for clarity). The lengths of axial and off-axis C–C bonds are labeled as b1 and b2, respectively.

tubes. Such a mutual arrangement may lead to this enlargement. As the IPs oscillate, the energies of the highest occupied molecular orbital (HOMO) also oscillate. We referred to Koopmans' theorem [27], which says that the energy required to remove an electron from an orbital is the negative of the orbital energy. The IP of a SWCNT is approximately the negative of the energy of its HOMO. It should be noted, that Koopmans'theorem does not offer an accurate description of either IP_v or IP_a, especially in the case of DFT calculations, in contrast to Hartree–Fock theory [28]. Therefore we used these values for the comparison purposes only. Having analyzed Table 1 data, we saw that the lower E(HOMO) of the SWCNTs the higher their IPs. Moreover, IP values fluctuate following E(HOMO) oscillations. It can be expected that the magnitude of fluctuations decreases upon a SWCNT elongation and tend to be zero in the case of infinite tubes.

In the earlier works, it was established that there are two different types of bonds in any SWCNT, axial b1 and off-axis b2 (Fig. 2) [29,30].

In those papers, the authors investigated b1 and b2 lengths, but did not mention about the bond lengths variation along the nanotubes [29,30]. The later work described the bond lengths alternation, but the change of lengths of whole SWCNTs was not stated [11]. Here, we determined the length of the SWCNT as a distance between the terminal carbon atoms on both tube ends. Further, in this work, we observed interesting behavior in the series of studied SWCNTs upon their ionization. The lengths of the following SWCNTs $C_{80}H_{20}$, $C_{140}H_{20}$, $C_{180}H_{20}$, and $C_{200}H_{20}$ slightly drop after ionization. These structures, except $C_{180}H_{20}$, can be assigned to an incomplete Clar network. Conversely, the remaining five of the studied SWCNTs becomes longer upon ionization. Fig. 3 shows the optimized lengths of b1 and b2 bonds for neutral $C_{80}H_{20}$ and $C_{100}H_{20}$, as well as their radical cations. We started counting b1 lengths from one end of a SWCNT to another, b2 bonds were adjacent to b1 ones. Thus, for example, for $C_{80}H_{20}$ (Fig. 2) we took into consideration seven b1 bonds and eight b2. A large bond alternation is observed for both b1 and b2 (Fig. 3).

Also, it can be seen evidently, that there is the anti-correlation of b1 and b2 assigned to a neutral tube and its radical cation. All the bond alternations were established to be symmetric relative to the tubes centers. One can observe a periodicity in the oscillations, but the plots are not simple and vary from one SWCNT to another. To understand different behavior of SWCNTs lengths upon ionization we implemented into consideration their HOMOs. It should be noted, they consist mainly of orbitals of carbon atoms, the hydrogen atoms at the tubes ends give little contribution to the frontier orbitals. As is depicted in Fig. 4, the HOMO of $C_{80}H_{20}$ is located around the circumference.

An electron removal cannot give a big impact in the b1 lengths increase, instead it give rise to an elongation of b2 bonds. In the

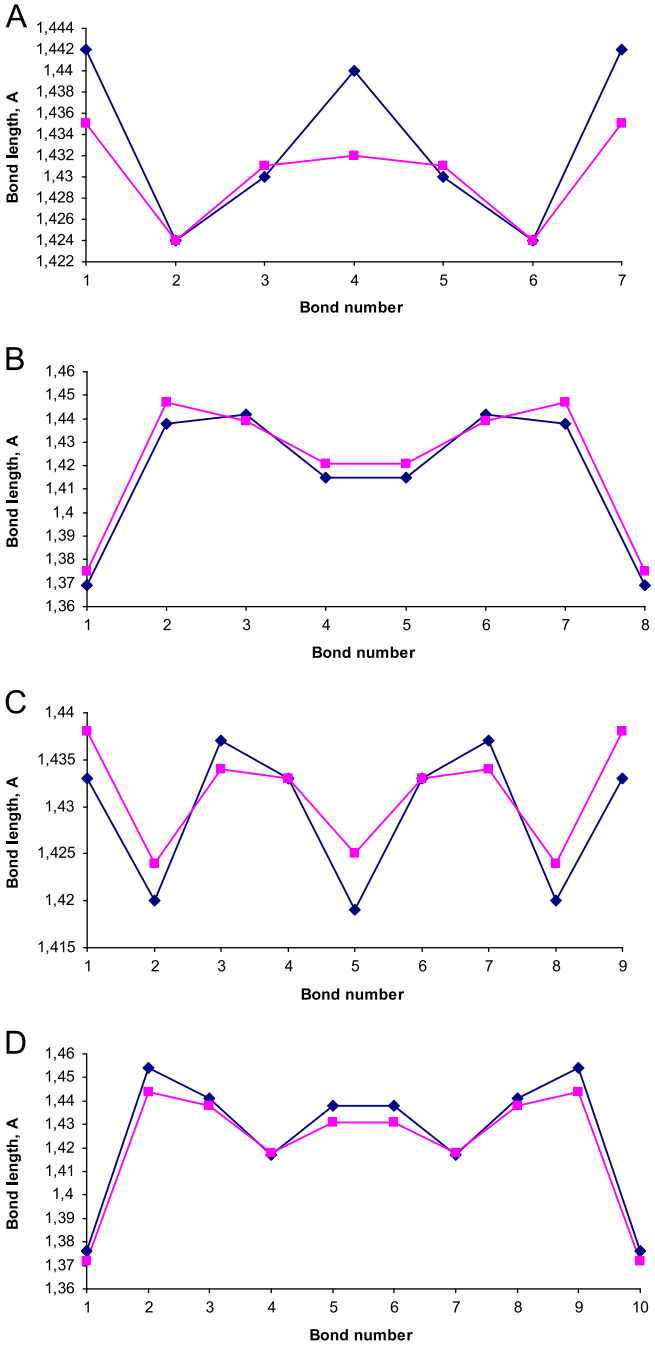

Fig. 3. Bond alternation vs. bond number. (A) ◆–b1 of $C_{80}H_{20}$, ■–b1 of $C_{80}H_{20}^{\bullet+}$; (B) ◆–b2 of $C_{80}H_{20}$, ■–b2 of $C_{80}H_{20}^{\bullet+}$; (C) ◆–b1 of $C_{100}H_{20}$, ■–b1 of $C_{100}H_{20}^{\bullet+}$ and (D) ◆–b2 of $C_{100}H_{20}$, ■–b2 of $C_{100}H_{20}^{\bullet+}$.

case of $C_{140}H_{20}$, $C_{180}H_{20}$, and $C_{200}H_{20}$, the HOMO localization as well as b1 and b2 behavior were the same. For these tubes a strip pattern appears, with circumferential areas of carbon atoms which give no contribution to the HOMOs. It is in the contrary with results of the Galano's work, in which it was declared that such a pattern appears only in the case of "long" tubes [15]. On the other hand, the HOMO of $C_{100}H_{20}$ is localized preferably axially (Fig. 4), and therefore an electron removal affects mainly on b1 bonds, making them longer. The resembling happens for $C_{20n}H_{20}$, $n=2$, 3, 5, 6, and 8. The data concern the differences between lengths of radical cations and neutral tubes (ΔL) were summarized in Table 1. The negative values reflect the fact that a radical cation is shorter than its neutral tube. Analyzing Table 1 data, we can see that absolute values of the elongation or the abridgement differ little.

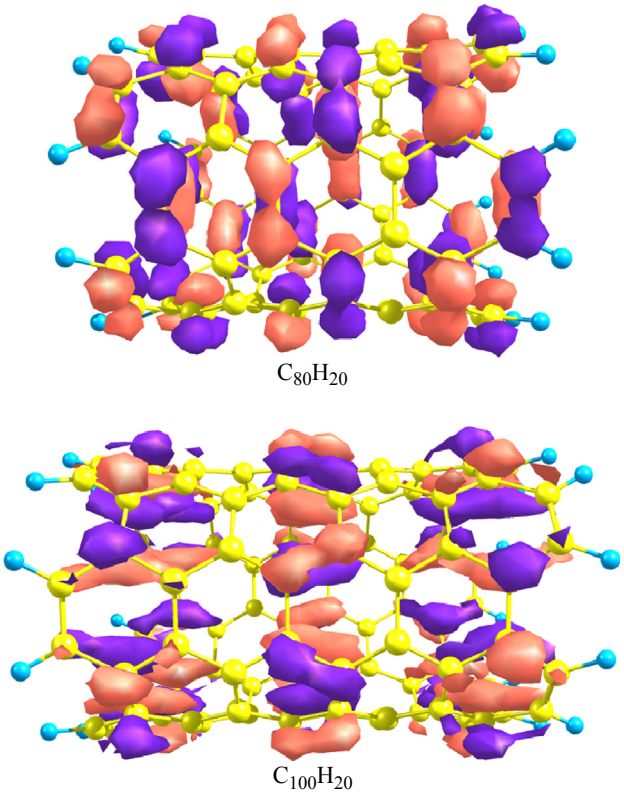

Fig. 4. HOMO plots of $C_{80}H_{20}$ and $C_{100}H_{20}$.

There are no evident oscillations of ΔL both for "short" and "long" SWCNTs. However, the relative lengths changes caused by an electron removal diminish on going to "long" tubes. It is not improbable, that in case of infinite tubes such a change will be insignificant, but upon review of finite length models this fact is of importance.

4. Conclusion

We investigated IP_v and IP_a for a series of SWCNTs as functions of the tube length by means of the DFT. Our calculations revealed that SWCNTs length, changing the local aromaticity periodically, affects their IPs values. Whereas "short" tubes demonstrate notable gap between IP_v and IP_a, "long" SWCNTs, for example $C_{200}H_{20}$, have similar IP_v and IP_a. It looks very possible, that in the case of real SWCNTs the both types of IPs become equal. It was established, that lengths of studied SWCNTs undergo a change upon ionization, and in the case of "short" tubes these relative changes are significant. This interesting effect of elongation or shortening, most probably, depends on the HOMO electron density distribution in SWCNTs.

Acknowledgment

Generous allotment of computational time from Computational Centre of Novosibirsk State University is gratefully acknowledged.

Appendix A. Supporting information

Supplementary data associated with this article can be found in the online version at http://dx.doi.org/10.1016/j.physe.2013.07.004.

References

[1] S. Iijima, T. Ichihashi, Nature 363 (1993) 603.
[2] M.M.J. Treacy, T.W. Ebbesen, J.M. Gibson, Nature 381 (1996) 678.
[3] V.N. Popov, Materials Science and Engineering R 43 (2004) 61.
[4] M. Baibarac, P. Gomez-Romero, Journal of Nanoscience and Nanotechnology 6 (2006) 289.
[5] A. Qureshi, W.P. Kang, J.L. Davidson, Y. Gurbuz, Diamond and Related Materials 18 (2009) 1401.
[6] M.S. Dresselhaus, G. Dresselhaus, A.M. Rao, P.C. Eklund, Synthetic Metals 78 (1996) 313.
[7] Y. Cheng, O Zhou, Comptes Rendus Physique 4 (2003) 1021.
[8] J.P. Sun, Z.X. Zhang, S.M. Hou, G.M. Zhang, Z.N. Gu, X.Y. Zhao, W.M. Liu, Z. Q. Xue, Applied Physics A 75 (2002) 479.
[9] I.K. Petrushenko, N.A. Ivanov, Fullerenes, Nanotubes and Carbon Nanostructures (2013) http://dx.doi.org/10.1080/1536383X.2012.684181, in press.
[10] A.V. Eletskii, Physics Uspekhi 52 (2009) 209.
[11] Z. Zhou, M. Steigerwald, M. Hybertsen, L. Brus, R.A. Friesner, Journal of the American Chemical Society 126 (2004) 3607.
[12] F. Buonocore, F. Trani, D. Ninno, A. Di Matteo, G. Cantele, G. Iadonisi, Nanotechnology 19 (2008) 025711.
[13] D.A. Buzatu, A.S. Biris, A.R. Biris, D.M. Lupu, J.A. Darsey, M.K. Mazumder, IEEE Transactions on Industry Applications 40 (2004) 1215.
[14] M. Baldoni, A. Sgamellotti, F. Mercuri, Chemical Physics Letters 464 (2008) 202.
[15] A. Galano, Chemical Physics 327 (2006) 159.
[16] P. Szakács, D. Kocsis, P.R. Surján, Journal of Chemical Physics 132 (2010) 034309.
[17] A.I. Murzashev, Russian Physics Journal 53 (2011) 1035.
[18] Y. Matsuo, K. Tahara, E. Nakamura, Organic Letters 5 (2003) 3181.
[19] F. Neese, ORCA – ab initio. Density Functional and Semiempirical Program Package, Universitat Bonn, 2009.
[20] A.D. Becke, Journal of Chemical Physics 98 (1993) 5648.
[21] C. Lee, W. Yang, R.G. Parr, Physical Review B 37 (1988) 785.
[22] R. Khorrampour, M.D. Esrafili, N.L. Hadipour, Physica E 41 (2009) 1373.
[23] E. Lewars, Computational Chemistry, Kluwer Academic Publishers, Peterborough, 2004.
[24] A. Schaefer, H. Horn, R.J. Ahlrichs, Journal of Chemical Physics 97 (1992) 2571.
[25] K. Eichkorn, O. Treutler, H. Ohm, M. Haser, R. Ahlrichs, Chemical Physics Letters 240 (1995) 283.
[26] K. Eichkorn, F. Weigend, O. Treutler, R. Ahlrichs, Theoretical Chemistry Accounts 97 (1997) 119.
[27] T. Koopmans, Physica 1 (1934) 104.
[28] C.-G. Zhan, J.A. Nichols, D.A. Dixon, Journal of Physical Chemistry A 107 (2003) 4184.
[29] K. Tanaka, H. Ago, T. Yamabe, K. Okahara, K. Okada, International Journal of Quantum Chemistry 63 (1997) 637.
[30] G.Y. Sun, J. Kurti, M. Kertesz, R.H. Baughman, Journal of Physical Chemistry B 107 (2003) 6924.